C. R. Mecanique 340 (2012) 900–909

Contents lists available at SciVerse ScienceDirect

Comptes Rendus Mecanique

www.sciencedirect.com

Out of Equilibrium Dynamics

Detonation-propelled shocks in tubular charges as a two-phase problem

Irina Brailovsky, Gregory Sivashinsky *

School of Mathematical Sciences, Tel Aviv University, Tel Aviv 69978, Israel

ARTICLE INFO

Article history:
Available online 13 November 2012

Keywords:
Detonation in tubular charges
Channel effect
Gas-permeable explosives

ABSTRACT

The article is concerned with the experimentally known phenomenon of the precursor shock driven by the detonation of a tubular charge. It is shown that the basic aspects of the effect may be successfully captured within a one-dimensional two-phase version of the Chapman–Jouguet (CJ) theory. A modified CJ principle for determination of the detonation and precursor shock velocities is discussed.

1. Introduction

Zeldovich [1], in his renowned paper of 1940 on the ZND model, asked a curious question: Can the gaseous detonation propel a precursor shock, as occurs in deflagrative combustion? This issue seems never to have enjoyed further discussion, presumably due to the realization that for the self-sustained CJ detonation higher speed precursor shocks are untenable (see Appendix A). It transpires, however, that for multiphase systems Zeldovich's question may well have a positive answer.

In 1947 Woodhead [2] reported an observation that detonation running through a solid charge with a longitudinal air-filled channel is accompanied by an air-shock propelled ahead of the detonation at a velocity around twice that of the detonation, Fig. 1. The emerging post-shock temperature is around 10,000 K, causing an intense luminosity of the shocked gas [2–5]. The gas flow developing in the channel is highly energetic (~ 10 km/s), which may be of practical interest, e.g. for launching small high-velocity projectiles [6,7] – an effective means for impact engineering [8].

Although there is now a substantial volume of literature on the subject [2–19], a first-principle understanding of the key interactions controlling the channel effect is still incomplete.

In the present study the problem is approached from the viewpoint that the tubular charge may be considered as a special case of a gas-permeable porous explosive. One therefore may expect that the channel effect should have a counterpart in the one-dimensional two-phase (gas–solid) picture widely employed in modeling of porous energetic materials. Indeed, as shown below the channel effect is quite generic to gas-permeable systems, and may be successfully captured even within the zero-reaction-zone CJ model. The familiar CJ principle of the minimum mass flux through the detonation, combined with the requirement of the maximum mass flux through the precursor shock, allows fixing both the detonation velocity as well as the velocity of the shock.

2. Formulation

Discarding transport effects, the set of conservation equations for the gas–solid mixture reads [20],

mass balance,

$$\frac{\partial}{\partial t}(\varphi_g\rho_g+\varphi_s\rho_s)+\frac{\partial}{\partial x}(\varphi_g\rho_g u_g+\varphi_s\rho_s u_s)=0 \tag{1}$$

* Corresponding author.
E-mail addresses: brailir@post.tau.ac.il (I. Brailovsky), grishas@post.tau.ac.il (G. Sivashinsky).

1631-0721/$ – see front matter
http://dx.doi.org/10.1016/j.crme.2012.10.037

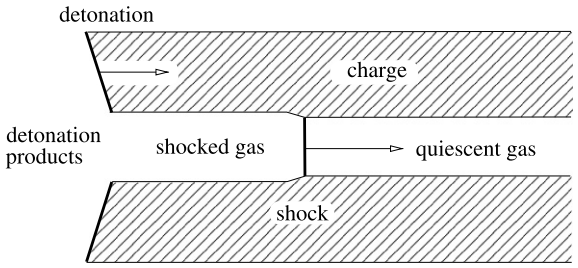

Fig. 1. Diagram for the channel effect. Arrows (also in Fig. 2) represent detonation and precursor shock velocities [5].

momentum balance,

$$\frac{\partial}{\partial t}(\varphi_g\rho_g u_g+\varphi_s\rho_s u_s)+\frac{\partial}{\partial x}\left(\varphi_g\rho_g u_g^2+\varphi_g P_g+\varphi_s\rho_s u_s^2+\varphi_s P_s\right)=0 \tag{2}$$

energy balance,

$$\frac{\partial}{\partial t}(\varphi_g\rho_g E_g+\varphi_s\rho_s E_s)+\frac{\partial}{\partial x}\left[\varphi_g u_g(\rho_g E_g+P_g)+\varphi_s u_s(\rho_s E_s+P_s)\right]=0 \tag{3}$$

$$E_g=e_g+\frac{1}{2}u_g^2,\qquad E_s=e_s+\frac{1}{2}u_s^2 \tag{4}$$

$$\varphi_g+\varphi_s=1 \tag{5}$$

Here the subscripts s and g refer to the solid and the gas phase, respectively. The state variables for the phases are: φ_g, φ_s – volume fractions; P_g, P_s – pressures; T_g, T_s – temperatures; ρ_g, ρ_s – densities; u_g, u_s – flow velocities; e_g, e_s – specific internal energies; E_g, E_s – total specific energies.

As in the CJ model, the reaction, converting the solid explosive into gaseous products, is assumed to occur instantly, i.e. detonation is treated as a reactive discontinuity. Hence, $\varphi_g=\varphi_0$, $\varphi_s=1-\varphi_0$ ahead of the detonation front, and $\varphi_g=1$, $\varphi_s=0$ in the products (φ_0 is prescribed).

To complete the formulation the following additional assumptions are made:

1. The solid phase is incompressible and static,

$$\rho_s=\rho_{s0},\qquad u_s=0 \tag{6}$$

2. Pressures in gas and solid phases are identical,

$$P_g=P_s=P \tag{7}$$

which is a common enough premise in modeling two-phase media [21]. By virtue of conditions (6), this assumption does not violate the hyperbolic character of the system.

3. Temperatures T_g and T_s are coupled through the relation,

$$T_s=T_0+k(T_g-T_0) \tag{8}$$

where T_0 is the ambient temperature, and k is the heat-exchange parameter. At $k=0$ the phases are thermally separated, while at $k=1$ the phases are in thermal equilibrium – an unlikely situation in supersonic combustion.

4. Equations of state for gas and solid phases are specified as,

$$e_g=c_g T_g,\qquad e_s=c_s T_s+Q \tag{9}$$

$$P=\left[\gamma(\varphi_g)-1\right]\rho_g e_g,\qquad \rho_s=\rho_{s0} \tag{10}$$

Here Q is the heat-release; c_g, c_s – specific heats, assumed to be constant; $\gamma(\varphi_g)$ – adiabatic index; $\gamma_p=\gamma(1)$, representing strongly pressurized detonation products, is about twice $\gamma_c=\gamma(\varphi_0)$ for the gas inside the channel.

5. To somewhat reduce mathematical clutter in the subsequent discussion it is set,

$$c_s=\gamma_c c_g\quad(=c_p) \tag{11}$$

For solid propellants such as cyclic nitramines RDX and HMX, c_s is slightly above c_p [22]. So the case of $c_s=c_p$ seems to be quite representative [23].

Ahead of the precursor shock,

$$P=P_0,\qquad \rho_g=\rho_{g0},\qquad T_g=T_0,\qquad u_g=u_{g0}=0,\qquad \varphi_g=\varphi_0 \tag{12}$$

Upon initiation and some transient time period the profiles of pressure, temperature, density, and flow-velocity are expected to assume simple step-like (though unsteady) structures as sketched in Fig. 2.

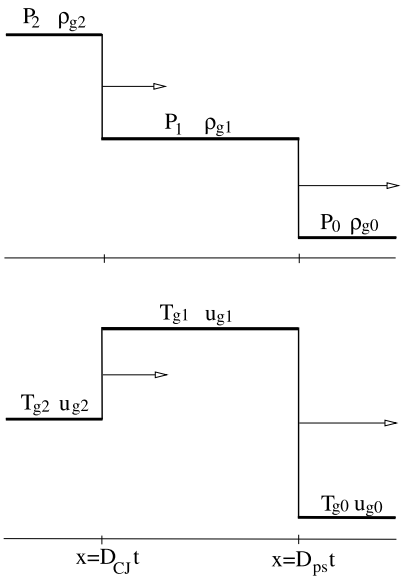

Fig. 2. Typical profiles of pressure/density, and temperature/flow-velocity in the channel effect; $u_{g0} = 0$. Proportions are not to scale.

3. Rayleigh and Rankine–Hugoniot relations

On the precursor shock ($x = D_{ps}t$), as implied by Eqs. (1)–(3), the following jump conditions are held (see also Fig. 2):

mass flux continuity,

$$\rho_{g1}(D_{ps} - u_{g1}) = \rho_{g0} D_{ps} \tag{13}$$

momentum flux continuity,

$$P_1 - \varphi_0 \rho_{g1} u_{g1}(D_{ps} - u_{g1}) = P_0 \tag{14}$$

energy flux continuity,

$$\varphi_0 \rho_{g1} E_{g1}(D_{ps} - u_{g1}) - \varphi_0 u_{g1} P_1 + D_{ps}(1 - \varphi_0)\rho_{s0} E_{s1} = \varphi_0 D_{ps} \rho_{g0} E_{g0} + D_{ps}(1 - \varphi_0)\rho_{s0} E_{s0} \tag{15}$$

where, by virtue of Eqs. (6)–(12),

$$E_{g0} = \frac{1}{\gamma_c - 1}\left(\frac{P_0}{\rho_{g0}}\right), \qquad E_{g1} = \frac{1}{\gamma_c - 1}\left(\frac{P_1}{\rho_{g1}}\right) + \frac{1}{2}u_{g1}^2 \tag{16}$$

$$E_{s0} = \frac{\gamma_c}{\gamma_c - 1}\left(\frac{P_0}{\rho_{g0}}\right) + Q\,, \qquad E_{s1} = \frac{\gamma_c(1-k)}{\gamma_c - 1}\left(\frac{P_0}{\rho_{g0}}\right) + \frac{\gamma_c k}{\gamma_c - 1}\left(\frac{P_1}{\rho_{g1}}\right) + Q \tag{17}$$

Here P_0, ρ_{g0}, E_{g0}, E_{s0} pertain to the state ahead of the advancing precursor shock, and P_1, ρ_{g1}, E_{g1}, E_{s1} – to the state behind the shock.

Similarly, on the detonation front ($x = Dt$) the associated jump conditions read,

mass flux continuity,

$$\rho_{g2}(D - u_{g2}) = \rho_a D \tag{18}$$

where

$$\rho_a = (1 - \varphi_0)\rho_{s0} + \varphi_0 \rho_{g1}\left(1 - \frac{u_{g1}}{D}\right) \tag{19}$$

is the apparent density;

momentum flux continuity,

$$P_2 - \rho_{g2} u_{g2}(D - u_{g2}) = P_1 - \varphi_0 \rho_{g1} u_{g1}(D - u_{g1}) \tag{20}$$

energy flux continuity,

$$\rho_{g2}E_{g2}(D-u_{g2})-u_{g2}P_2=\varphi_0\rho_{g1}E_{g1}(D-u_{g1})-\varphi_0 u_{g1}P_1+D(1-\varphi_0)\rho_{s0}E_{s1} \tag{21}$$

where

$$E_{g2}=\frac{1}{\gamma_p-1}\left(\frac{P_2}{\rho_{g2}}\right)+\frac{1}{2}u_{g2}^2 \tag{22}$$

For the precursor shock Eqs. (13)–(17) may be recast into the form of the equivalent Rayleigh and Rankine–Hugoniot (RRH) relations,

$$P_1=P_0+\varphi_0\rho_{g0}D_{ps}^2\left(1-\frac{\rho_{g0}}{\rho_{g1}}\right) \tag{23}$$

$$P_1\left[\frac{\rho_{g0}}{\rho_{g1}}\left(\frac{\gamma_c+1-2\gamma_c(1-\varphi_0)}{\gamma_c-1}\right)+\frac{2k\gamma_c\rho_{s0}(1-\varphi_0)}{\rho_{g1}(\gamma_c-1)}+2(1-\varphi_0)-1\right]$$
$$=P_0\left[\frac{\gamma_c+1-2(1-\varphi_0)}{\gamma_c-1}-\frac{\rho_{g0}}{\rho_{g1}}+\frac{2k\gamma_c\rho_{s0}(1-\varphi_0)}{\rho_{g0}(\gamma_c-1)}\right] \tag{24}$$

$$u_{g1}=D_{ps}\left(1-\frac{\rho_{g_0}}{\rho_{g_1}}\right) \tag{25}$$

For the detonation the RRH relations, implied by Eqs. (18)–(22), read,

$$P_2=P_1+D^2\rho_a\left(1-\frac{\rho_a}{\rho_{g2}}\right)+\varphi_0\rho_{g1}u_{g1}(u_{g1}-D) \tag{26}$$

$$P_2\left[\frac{\rho_a}{\rho_{g2}}\left(\frac{\gamma_p+1}{\gamma_p-1}\right)-1\right]=P_1\left[\frac{\gamma_c+1-2(1-\varphi_0)}{\gamma_c-1}-\frac{\rho_a}{\rho_{g2}}-\frac{2\gamma_c\varphi_0}{\gamma_c-1}\left(\frac{u_{g1}}{D}\right)\right]$$
$$+\varphi_o\rho_{g1}u_{g1}(u_{g1}-D)\left(1-\frac{\rho_a}{\rho_{g2}}-\frac{u_{g1}}{D}\right)+2\rho_{s0}(1-\varphi_0)(Q+c_sT_{s1}) \tag{27}$$

$$u_{g2}=D\left(1-\frac{\rho_a}{\rho_{g2}}\right) \tag{28}$$

4. Precursor-free mode

As in a single-phase non-reactive gaseous system the RRH relations (23), (24) yield two possible solutions for ρ_{g1}. The first,

$$\rho_{g1}=\rho_{g0} \tag{29}$$

and the second, defined by the relation,

$$\rho_{g1}\left[\frac{2\gamma_c\varphi_0}{\gamma_c-1}+\frac{\varphi_0\rho_{g0}D_{ps}^2(1-2(1-\varphi_0))}{P_0}+\frac{2k\gamma_c\rho_{s0}(1-\varphi_0)}{\rho_{g0}(\gamma_c-1)}\right]$$
$$=\frac{\varphi_0\rho_{g0}^2D_{ps}^2}{P_0}\left[\frac{\gamma_c+1-2\gamma_c(1-\varphi_0)}{\gamma_c-1}+\frac{2k\gamma_c\rho_{s0}(1-\varphi_0)}{\rho_{g0}(\gamma_c-1)}\right] \tag{30}$$

The first solution pertains to the precursor-free mode where $P_1=P_0$, $T_{g1}=T_0$, $u_{g1}=0$, and D_{ps} therefore drops out of the model. In this case for the minimum possible detonation velocity (CJ regime), as one would anticipate,

$$D_{CJ}-u_{g2}=\sqrt{\gamma_pP_2/\rho_{g2}} \tag{31}$$

which is the sonic velocity in the products, and

$$D_{CJ}\simeq\sqrt{2\left(\gamma_p^2-1\right)(Q+c_sT_0)} \tag{32}$$

provided $P_2\gg P_0$ and $\rho_{s0}\gg\rho_{g0}$.

Up to the augmented heat-release and enhanced adiabatic index the situation is therefore similar to that of conventional gaseous detonation.

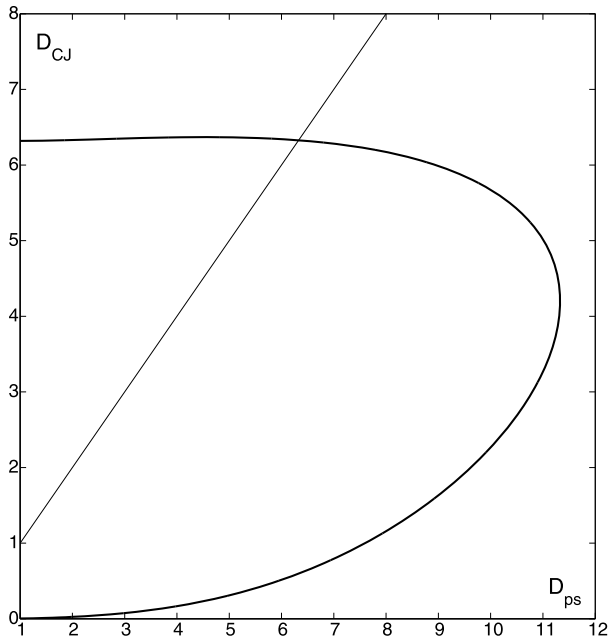

Fig. 3. $\hat{D}_{CJ}$ vs. $\hat{D}_{ps}$ dependency calculated for $\gamma_p = 3$, $\gamma_c = 1.4$, $\sigma = 0.1$, $\alpha = 20{,}000(1-\varphi_0)$, $\varphi_0 = 0.6$, $k = 0$. In all the figures, the hats on the labels have been omitted, and the straight line represents the separatrix $\hat{D}_{CJ} = \hat{D}_{ps}$.

For further discussion it is convenient to deal with scaled variables and parameters,

$$\hat{P} = P/P_0, \qquad \hat{T}_g = T_g/T_b, \qquad \hat{\rho}_g = \rho_g/\rho_b, \qquad \hat{u}_g = u_g/a_b$$
$$\hat{D} = D/a_b, \qquad \hat{D}_{ps} = D_{ps}/a_b, \qquad \sigma = T_0/T_b, \qquad \alpha = \rho_{s0}(1-\varphi_0)/\rho_b$$

Here,

$$T_b = T_0 + Q/c_p, \qquad \rho_b = P_0/c_g T_b(\gamma_c - 1), \qquad a_b = \sqrt{\gamma_c P_0/\rho_b}$$

are the burned gas temperature, density and sonic velocity pertaining to isobaric deflagrative combustion.

For a set of parameters,

$$\gamma_c = 1.4, \qquad \gamma_p = 3, \qquad \sigma = 0.1, \qquad \alpha = 20{,}000(1-\varphi_0), \qquad \varphi_0 = 0.6$$

which may correspond, for example, to

$$P_0 = 1 \text{ atm}, \qquad T_0 = 293 \text{ K}, \qquad T_b = 2930 \text{ K}, \qquad \rho_{g0} = 0.001 \text{ g/cm}^3$$
$$\rho_b = 0.0001 \text{ g/cm}^3, \qquad \rho_{s0} = 2 \text{ g/cm}^3, \qquad a_b = 1172 \text{ m/s}$$

calculation of the precursor-free CJ detonation yields,

$$\hat{D}_{CJ} = 6.322 \text{ (7409 m/s)}, \qquad \hat{P}_2 = 112{,}006 \text{ (113 kbar)}, \qquad \hat{\rho}_{g2} = 10{,}675 \left(1 \text{ g/cm}^3\right)$$
$$\hat{u}_{g2} = 1.581 \text{ (1854 m/s)}, \qquad \hat{T}_{g2} = 2.1 \text{ (6152 K)}$$

which are in a reasonable enough range.

5. Precursor shock

Taking the precursor shock velocity D_{ps} as a prescribed parameter, Eqs. (23), (24), (30) determine P_1, ρ_{g1}, T_{g1}, u_{g1} as functions of D_{ps}. This, in turn, uniquely defines the RRH relations (26), (27) for calculation of the CJ detonation.

Fig. 3 shows the $\hat{D}_{CJ}(\hat{D}_{ps})$ dependency evaluated for the CJ tangency solution (minimum/maximum possible $\hat{D}$ for a given $\hat{D}_{ps}$) at $k = 0$. Other parameters employed are identical to those of Section 4. Thus, there is a whole family of solutions with $\hat{D}_{CJ} < \hat{D}_{ps}$ representing CJ detonations furnished with precursor shocks.

A somewhat unexpected feature of the emerging $\hat{D}_{CJ}(\hat{D}_{ps})$ dependency is the turning point (maximum $\hat{D}_{ps}$) beyond which the solution for $\hat{D}_{CJ}$ ceases to exist. It seems natural to suggest that this turning-point-solution is precisely the one

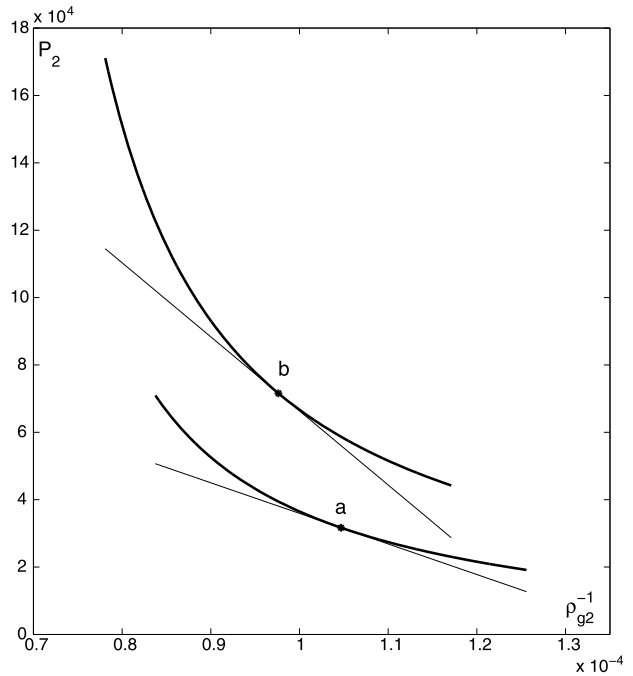

Fig. 4. Hugoniot curves (bold) and Rayleigh lines (thin) calculated for the tangency (CJ) solutions at $\hat{D}_{ps} = 11$ near the turning point ($\hat{D}_{ps} = 11.32$, $\hat{D}_{CJ} = 4.347$). At the lower (a) and upper (b) CJ points $\hat{D}_{CJ} = 3.266$ and 5.016, respectively.

realized physically.[1] Validation of this conjecture presumably may be attained through appropriate stability analysis, or high-resolution numerical simulations, accounting for the reaction-zone structure and transport effects[2] (see also Appendix A).

Fig. 4 shows the Hugoniot curves and Rayleigh lines (26), (27) of the tangency (CJ) solutions near the turning point. In the two-phase problem the Hugoniot curve for the products depends on the flame velocity D. As a result, the upper and lower tangency (CJ) points, for a given D_{ps}, belong to different Hugoniot curves. This, in turn, allows merging of the upper and lower branches of the $\hat{D}_{CJ}(\hat{D}_{ps})$ curves at the turning point. In conventional single-phase systems the gap between the upper and lower tangency points is unbridgeable.

Within the $\hat{D}_{CJ}(\hat{D}_{ps})$ bubble the Hugoniot and Rayleigh lines do not intersect. Similar to single-phase systems, the upper/lower branch of the $\hat{D}_{CJ}(\hat{D}_{ps})$ curve corresponds to the minimum/maximum possible $\hat{D}$.

At the turning point,

$$\begin{aligned}
&\hat{D}_{ps} = 11.32\,(13{,}267\ \text{m/s}), && \hat{D}_{CJ} = 4.347\,(5095\ \text{m/s})\\
&\hat{P}_1 = 803\,(0.811\ \text{kbar}), && \hat{P}_2 = 54{,}388\,(54.932\ \text{kbar})\\
&\hat{\rho}_{g1} = 157\,\big(0.016\ \text{g/cm}^3\big), && \hat{\rho}_{g2} = 10{,}026\,\big(1\ \text{g/cm}^3\big)\\
&\hat{u}_{g1} = 10.599\,(12{,}422\ \text{m/s}), && \hat{u}_{g2} = 0.937\,(1098\ \text{m/s})\\
&\hat{T}_{g1} = 5.122\,(15{,}007\ \text{K}), && \hat{T}_{g2} = 1.085\,(3179\ \text{K})\\
&\hat{D}_{CJ} - \hat{u}_{g2} = \sqrt{\gamma_p \hat{P}_2/\gamma_c \hat{\rho}_{g2}}
\end{aligned} \tag{33}$$

which is a scaled version of Eq. (31).

The post-shock flow-velocity u_{g1} exceeds D_{CJ}. So a part of the detonation products enters the channel. Note that while the total mass flux of the gas–solid mixture is certainly conserved, this does not hold for the mass flux of the gas (due to gasification of the charge).

The temperature in the shocked gas T_{g1} is significantly higher than in the products T_{g2}. This outcome is perfectly in line with experimental observations that the intense post-shock luminosity does not extend over the products [2,18,19].

[1] An alternative condition $u_{g1} = D$ [5,18,19] (impermeable piston assumption) brings D_{ps} very close to D, which leaves a substantial body of experimental data uncovered [5].

[2] The experience with other physical systems having similar non-uniqueness [24] shows that to ensure a 'natural selection' even minute dissipative effects may be important.

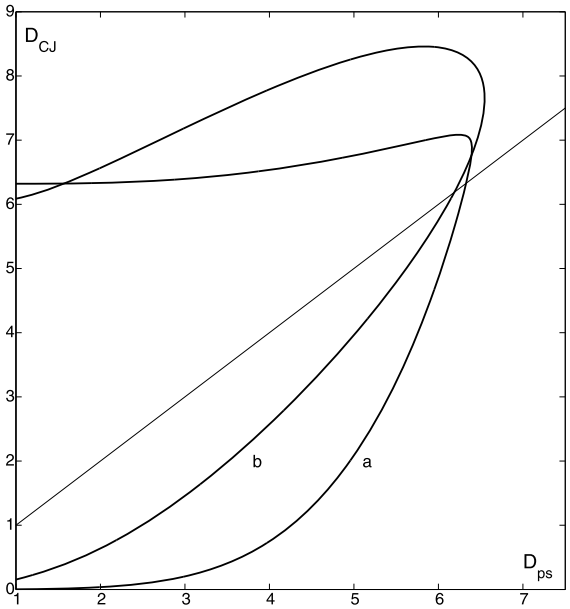

Fig. 5. $\hat{D}_{CJ}$ vs. $\hat{D}_{ps}$ dependency calculated for $\varphi_0 = 0.496$ (a) and 0.99 (b). For other conditions see the caption for Fig. 3.

As one would expect, the hydrodynamic profiles corresponding to the lower part of the $\hat{D}_{CJ}(\hat{D}_{ps})$ curve are deflagration-like, provided $\hat{D}_{ps}$ is low enough. For example, at $\hat{D}_{ps} = 0.5$: $\hat{D}_{CJ} = 0.0002$, $\hat{P}_1 = 1.26$, $\hat{P}_2 = 0.39$, $\hat{\rho}_{g1} = 14.55$, $\hat{\rho}_{g2} = 0.045$, $\hat{u}_{g1} = 0.16$, $\hat{u}_{g2} = -4.30$, $\hat{T}_{g1} = 0.09$, $\hat{T}_{g2} = 1.72$.

For sufficiently high and low porosities ($\varphi_0 < \varphi_{0,min} = 0.498$ and $\varphi_0 > \varphi_{0,max} = 0.97$) the turning point crosses the separatrix $\hat{D}_{CJ} = \hat{D}_{ps}$, ending up in the unphysical domain $\hat{D}_{CJ} > \hat{D}_{ps}$ (Fig. 5). This outcome is qualitatively in line with experimental observations. According to Refs. [9,16,18], both for high and low porosities the channel effect disappears and the conventional precursor-free regime becomes a preferable mode.

Note that under further reduction of φ_0 the turning point escapes to infinity resulting in the break up of the $\hat{D}_{CJ}(\hat{D}_{ps})$ curve.

For the adopted formulation the lower threshold $\varphi_{0,min} = 0.498$ is relatively high. It may however be lowered by replacing the pressure equilibrium condition (7) by $P_s - P_0 = \beta(P_g - P_0)$ with $\beta < 1$, presumably more adequate for gas–solid systems in question [14,21].

Accounting for the heat exchange ($k > 0$) weakens the channel effect – the disparity between D_{CJ} and D_{ps}, and T_{g1} and T_{g2} is diminished (Fig. 6). For example, for $k = 0.001$ at the turning point,

$$\hat{D}_{ps} = 8.69\,(10{,}185\ \text{m/s}), \qquad \hat{D}_{CJ} = 4.688\,(5494\ \text{m/s})$$
$$\hat{P}_1 = 568\,(0.574\ \text{kbar}), \qquad \hat{P}_2 = 62{,}909\,(63.538\ \text{kbar})$$
$$\hat{\rho}_{g1} = 408.449\,\left(0.004\ \text{g/cm}^3\right), \qquad \hat{\rho}_{g2} = 9923\,\left(0.99\ \text{g/cm}^3\right)$$
$$\hat{u}_{g1} = 8.477\,(9935\ \text{m/s}), \qquad \hat{u}_{g2} = 1.002\,(1174\ \text{m/s})$$
$$\hat{T}_{g1} = 1.391\,(4076\ \text{K}), \qquad \hat{T}_{g2} = 1.268\,(3715\ \text{K})$$

It is curious that formally self-sustained gasification waves may well survive even in the absence of chemical heat-release ($Q = 0$, $\sigma = 1$), Fig. 7.

$$\hat{D}_{ps} = 22.98\,(8525\ \text{m/s}), \qquad \hat{D}_{CJ} = 3.919\,(1454\ \text{m/s})$$
$$\hat{P}_1 = 331\,(0.334\ \text{kbar}), \qquad \hat{P}_2 = 44{,}072\,(44.513\ \text{kbar})$$
$$\hat{\rho}_{g1} = 15.277\,\left(0.015\ \text{g/cm}^3\right), \qquad \hat{\rho}_{g2} = 10{,}301\,\left(10.301\ \text{g/cm}^3\right)$$
$$\hat{u}_{g1} = 21.476\,(7323\ \text{m/s}), \qquad \hat{u}_{g2} = 0.891\,(331\ \text{m/s})$$
$$\hat{T}_{g1} = 21.671\,(6350\ \text{K}), \qquad \hat{T}_{g2} = 0.856\,(251\ \text{K})$$

Here $P_0 = 1$ atm, $T_b = T_0 = 293$ K, $\rho_b = \rho_0 = 0.001$ g/cm^3, $a_b = a_0 = 371$ m/s.

A similar effect has recently been identified in the problem of conductive/convective burning of gas-permeable explosives [25].

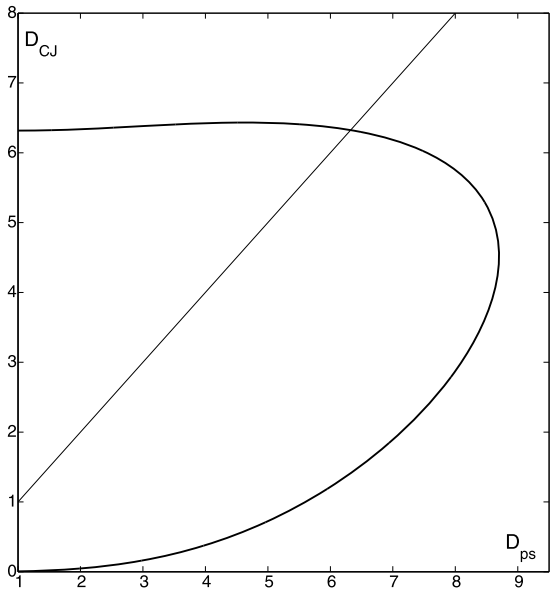

Fig. 6. $\hat{D}_{CJ}$ vs. $\hat{D}_{ps}$ dependency calculated for $k = 0.001$. For other conditions see the caption for Fig. 3.

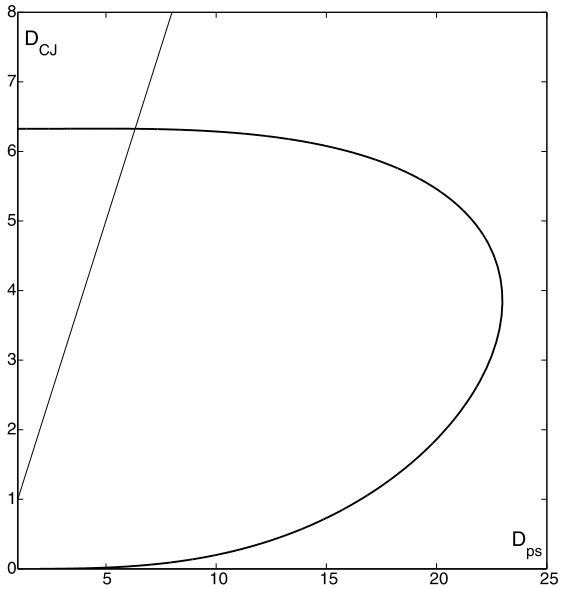

Fig. 7. $\hat{D}_{CJ}$ vs. $\hat{D}_{ps}$ dependency calculated for $\sigma = 1$. For other conditions see the caption for Fig. 3.

The channel effect also survives the distinguished limit combining high porosity ($\varphi_0 \to 1$) with strong disparity between gas/solid densities ($\rho_{s0}/\rho_b \to \infty$), while keeping the product $\alpha = (\rho_{s0}/\rho_b)(1 - \varphi_0)$ finite. This limit leads to considerable simplifications of the equations, which may be advantageous for theoretical explorations.

6. Concluding remarks

The present study demonstrates the compatibility of detonation-propelled shocks with the general thermodynamics of gas-permeable systems. However, it does not explain why and when the precursor mode (when it is allowed) is physically favored over the invariably present precursor-free mode. This issue needs further exploration.

In the proposed model the turning-point detonation (Section 5) appears to be slower than that for the gas-impermeable cast explosive ($\varphi_0 = 0$, $\hat{D}_{CJ} = 6.325$). Experimentally however, the situation is just the opposite: the detonation velocity is enhanced by the channeling [2,4,5]. There are at least two major, and possibly related, ingredients unaccounted for in the model which could be partially responsible for this discrepancy: (i) the conical profile of the detonation front in tubular

charges, increasing its apparent velocity [4,18,19]; and (ii) compression induced lateral density increase within the shocked part of the charge [5] – known to raise the detonation velocity.

The present model therefore definitely needs an enhancement. Yet whatever future shape it might take, the topology of the found $\hat{D}_{CJ}(\hat{D}_{ps})$ dependency, being based on fundamental principles, is unlikely to be altered.

On the other hand, if the tubular charge is replaced by a powdered charge of the same average density the resulting detonation velocity may well fall considerably below that for the compact explosive [5, p. 30], which is qualitatively in line with predictions of the current 1D model. In this case the detonation is likely to be preceded by a spontaneous channeling of the powder [17], rather than its usual uniform compaction.

Acknowledgements

This paper is dedicated to Paul Clavin on the occasion of his 70th birthday as a token of friendship, and in admiration of his contribution to combustion theory. The authors would like to express their deepest gratitude to Ash Kapila for pointing out an omission in one of the equations in the original version of the paper. They would also like to thank Leonid Kagan and Peter Gordon for many engaging discussions. These studies were supported by the US–Israel Binational Science Foundation (Grant 2006-151) and the Israel Science Foundation (Grant 32/09).

Appendix A. Zeldovich's problem

In the conventional gaseous detonation, assuming γ to be constant, the RRH relations for the precursor shock and detonation read,

precursor shock,

$$P_1 = P_0 + D_{ps}^2\rho_0\left(1-\frac{\rho_0}{\rho_1}\right) \tag{A.1}$$

$$P_1\left[\frac{\rho_0}{\rho_1}\left(\frac{\gamma+1}{\gamma-1}\right)-1\right] = P_0\left(\frac{\gamma+1}{\gamma-1}-\frac{\rho_0}{\rho_1}\right) \tag{A.2}$$

$$u_1 = D_{ps}\left(1-\frac{\rho_0}{\rho_1}\right) \tag{A.3}$$

detonation,

$$P_2 = P_1 + D^2\rho_a\left(1-\frac{\rho_a}{\rho_2}\right) + \rho_1 u_1(u_1-D) \tag{A.4}$$

$$P_2\left[\frac{\rho_a}{\rho_2}\left(\frac{\gamma+1}{\gamma-1}\right)-1\right] = P_1\left[\frac{\gamma+1}{\gamma-1}-\frac{\rho_a}{\rho_2}-\frac{2\gamma}{\gamma-1}\left(\frac{u_1}{D}\right)\right] + \rho_1 u_1(u_1-D)\left(1-\frac{\rho_a}{\rho_2}-\frac{u_1}{D}\right) + 2\rho_1 Q\left(1-\frac{u_1}{D}\right) \tag{A.5}$$

$$u_2 = D\left(1-\frac{\rho_a}{\rho_2}\right) \tag{A.6}$$

where

$$\rho_a = \rho_1\left(1-\frac{u_1}{D}\right) \tag{A.7}$$

is the apparent density.

Eqs. (A.1), (A.2) yield two possible solutions for ρ_1. The first one, $\rho_1 = \rho_0$, pertains to the conventional precursor-free detonation. The second solution is defined by the relation,

$$\rho_1\left(\frac{\gamma+1}{\gamma-1}+\frac{D_{ps}^2\rho_0}{P_0}+1\right) = \frac{D_{ps}^2\rho_0^2}{P_0}\left(\frac{\gamma+1}{\gamma-1}\right) \tag{A.8}$$

Fig. A.1 shows the $\hat{D}_{CJ}(\hat{D}_{ps})$ dependency calculated for the CJ tangency solutions. The upper curve pertains to the upper tangency solution (CJ detonation), and the lower curve – to the lower tangency solution (CJ deflagration). For the CJ detonation D_{CJ} appears to be higher than D_{ps}, i.e. the precursor shock is ruled out. However for the CJ deflagration and sufficiently small D_{ps} the precursor shocks are quite feasible.

The maximum possible D_{ps}, where

$$D_{CJ} = D_{ps} = \sqrt{(\gamma^2-1)Q/2} + \sqrt{(\gamma^2-1)Q/2 + \gamma P_0/\rho_0} \tag{A.9}$$

corresponds to the classical CJ detonation. But here it appears as a CJ deflagration of the shocked premixture.

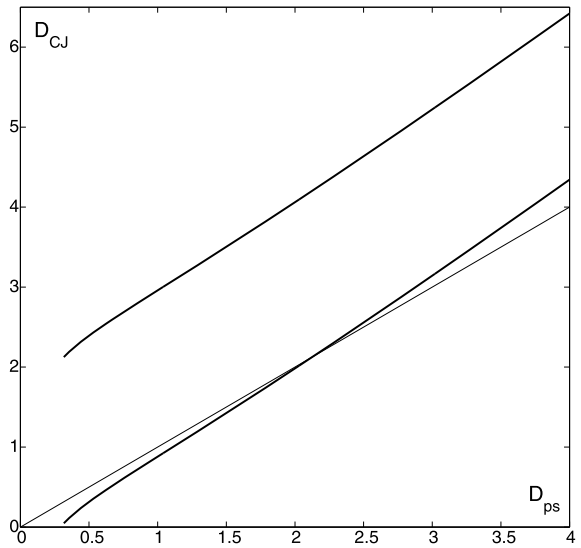

Fig. A.1. $\hat{D}_{CJ}$ vs. $\hat{D}_{ps}$ dependency for gaseous system calculated for $\gamma = 1.4$, $\sigma = 0.1$. The reference scales employed are identical to those of Section 4.

At $D_{CJ} = D_{ps}$ the deflagration and the precursor shock form a steady complex. Within the adopted formulation, however, the gap between the reactive and shock interfaces remains undetermined.

Depending on whether the adopted formulation allows for the precursor shocks or not, the same propagation velocity D_{CJ} may occur either within the deflagrative or within the detonative set of solutions.

In the precursor shock formulation the detonation velocity D_{CJ} corresponds to the maximum D_{ps}. This lends extra weight to the selection principle suggested for the two-phase problem.

References

[1] Ya.B. Zeldovich, On the theory of the propagation of detonation in gaseous systems, Sov. J. Exp. Theor. Phys. 10 (1940) 542–568.
[2] D.W. Woodhead, Velocity of detonation of a tubular charge of explosive, Nature 160 (1947) 644.
[3] D.W. Woodhead, Advance detonation in a tubular charge of explosive, Nature 183 (1959) 1756–1757.
[4] D.W. Woodhead, H. Titman, Detonation phenomena in a tubular charge of explosive, Explosivstoffe 13 (1965) 113–123, 141–155.
[5] C.H. Johansson, P.A. Persson, Detonics of High Explosives, Academic Press, London, 1970.
[6] V.M. Titov, G.A. Shvetsov, Laboratory methods of launching projectiles by means of shaped charges, Combust. Expl. Shock Waves 6 (1969) 349–351.
[7] P.A. Lasorskii, A.V. Plastinin, V.V. Sil'vestrov, V.M. Titov, Acceleration of solid particles during cumulation of detonation products in vacuum, Combust. Expl. Shock Waves 35 (1999) 443–446.
[8] L.E. Fugelso, J.N. Albright, G.C. Langer, K.L. Burns, A hypervelocity projectile launcher for well perforation, Int. J. Impact Eng. 10 (1990) 171–184.
[9] L.V. Dubnov, L.D. Khotina, Channel effect mechanism in the detonation of condensed explosives, Combust. Expl. Shock Waves 2 (1966) 59–63.
[10] H. Ahrens, Über den detonationsvorgang bei zylindrischen sprengstoffadungen mit axialer höhlung, Explosivstoffe 13 (1965) 124–134, 155–164, 180–198, 267–276, 295–309;
H. Ahrens, Über den detonationsvorgang bei zylindrischen sprengstoffadungen mit axialer höhlung, Explosivstoffe 15 (1967) 121–129, 145, 175–185.
[11] A.S. Zagumennov, N.S. Titova, Yu.I. Fadeenko, V.P. Chistyakov, Detonation of elongated charges with cavities, Sov. J. Appl. Mech. Tech. Phys. 10 (1969) 246–250.
[12] V.V. Mitrofanov, Ultra-speed detonation in charges with longitudinal channels, Combust. Expl. Shock Waves 11 (1975) 63–79.
[13] I.T. Bakirov, V.V. Mitrofanov, High-velocity two-layer detonation in an explosive-gas system, Sov. Phys. Dokl. 21 (1976) 704–706.
[14] V.V. Mitrofanov, Detonation in two-layer systems, Acta Astronaut. 3 (1976) 995–1004.
[15] M. Held, Influence of longitudinal gaps on the detonation front, Propellants Explos. Pyrotech. 20 (1995) 170–177.
[16] F. Sumiya, K. Tokita, M. Nakano, Y. Ogata, Y. Wada, M. Seto, K. Katsuyama, S. Ito, Experimental study of the channel effect in emulsion explosives, J. Mater. Process. Technol. 85 (1999) 25–29.
[17] M.J. Gifford, K. Tsembelis, J.E. Field, Anomalous detonation velocities following type II deflagration-to-detonation transition in pentaerythritol tetranitrate, J. Appl. Phys. 91 (2002) 4995–5001.
[18] V. Tanguay, A.J. Higgins, The high-explosive channel effect: Influence of boundary layers on the precursor shock wave in air, J. Appl. Phys. 95 (2004) 6159–6166.
[19] V. Tanguay, A.J. Higgins, The channel effect: Coupling of the detonation and the precursor shock wave by precompression of the explosive, J. Appl. Phys. 96 (2004) 894–4902.
[20] A.K. Kapila, R. Menikoff, J.B. Bdzil, S.F. Son, D.S. Stewart, Two-phase modeling of deflagration-to-detonation transition in granular materials: Reduced equations, Phys. Fluids 13 (2001) 3002–3024.
[21] R.I. Nigmatulin, Dynamics of Multiphase Media, Hemisphere, New York, 1991.
[22] A.A. Zenin, Study of combustion mechanism of nitramine–polymer mixtures, Final Tech. Rep. 1999012214, European Research Office of the US Army, Contract N68171-97-M-5771, Nov. 1998.
[23] T. Mitani, F.A. Williams, A model for the deflagration of nitramines, Proc. Combust. Inst. 21 (1986) 1965–1974.
[24] H. Berestycki, L. Kagan, S. Kamin, G. Sivashinsky, Metastable behaviour for premixed gas flames propagating through rectangular channels, Interfaces Free Bound. 6 (2004) 423–438.
[25] L.S. Kagan, S.B. Margolis, G.I. Sivashinsky, Modelling of the transition from conductive to convective burning in porous energetic materials, Combust. Theory Model. 16 (2012) 737–746.